

## Supplementary Information

### Tree-like Nanoporous WO<sub>3</sub> Photoanode with Enhanced Charge Transport Efficiency for Photoelectrochemical Water Oxidation

*Sun Shin<sup>a,d,1</sup>, Hyun Soo Han<sup>a,b,1</sup>, Ju Seong Kim<sup>a</sup>, Ik Jae Park<sup>a</sup>, Myeong Hwan Lee<sup>a</sup>, Kug Sun Hong<sup>a</sup> and In Sun Cho<sup>c,\*</sup>*

<sup>a</sup>Department of Materials Science and Engineering, Seoul National University, Seoul 151-744, Korea

<sup>b</sup>Department of Mechanical Engineering, Stanford University, Stanford, CA 94306, United States

<sup>c</sup>Department of Materials Science and Engineering & Energy Systems Research, Ajou University, Suwon 443-749, Korea

<sup>d</sup>Engineering Research Institute, Ajou University, Suwon 443-749, Korea

Corresponding Author:

E-mail: [insuncho@ajou.ac.kr](mailto:insuncho@ajou.ac.kr)

[<sup>1</sup>] These authors contributed equally to this work.

**Table S1.** Calculated nanocrystals sizes in the WO<sub>3</sub> photoanodes synthesized at various oxygen partial pressures (W-100: 100 mTorr, W-300: 300mTorr, and W-600: 600 mTorr), which is estimated from Scherrer equation using (002) reflection peak.

	$\lambda$ (nm)	$\beta$ (rad)	$\theta_B$	Size (nm)
W-100	0.154	$2.48 \cdot 10^{-3}$	12.1848	<b>57.2</b>
W-300	0.154	$2.83 \cdot 10^{-3}$	12.1848	<b>53.3</b>
W-600	0.154	$2.412 \cdot 10^{-3}$	12.1848	<b>58.7</b>

$$\tau = \frac{0.9\lambda}{\beta \cos \theta_B},$$

$\tau$  is the mean size of the crystallite;

$\lambda$  is the X-ray wavelength;

$\beta_B$  is the line broadening at half the maximum intensity in radian

$\theta$  is the Bragg angle

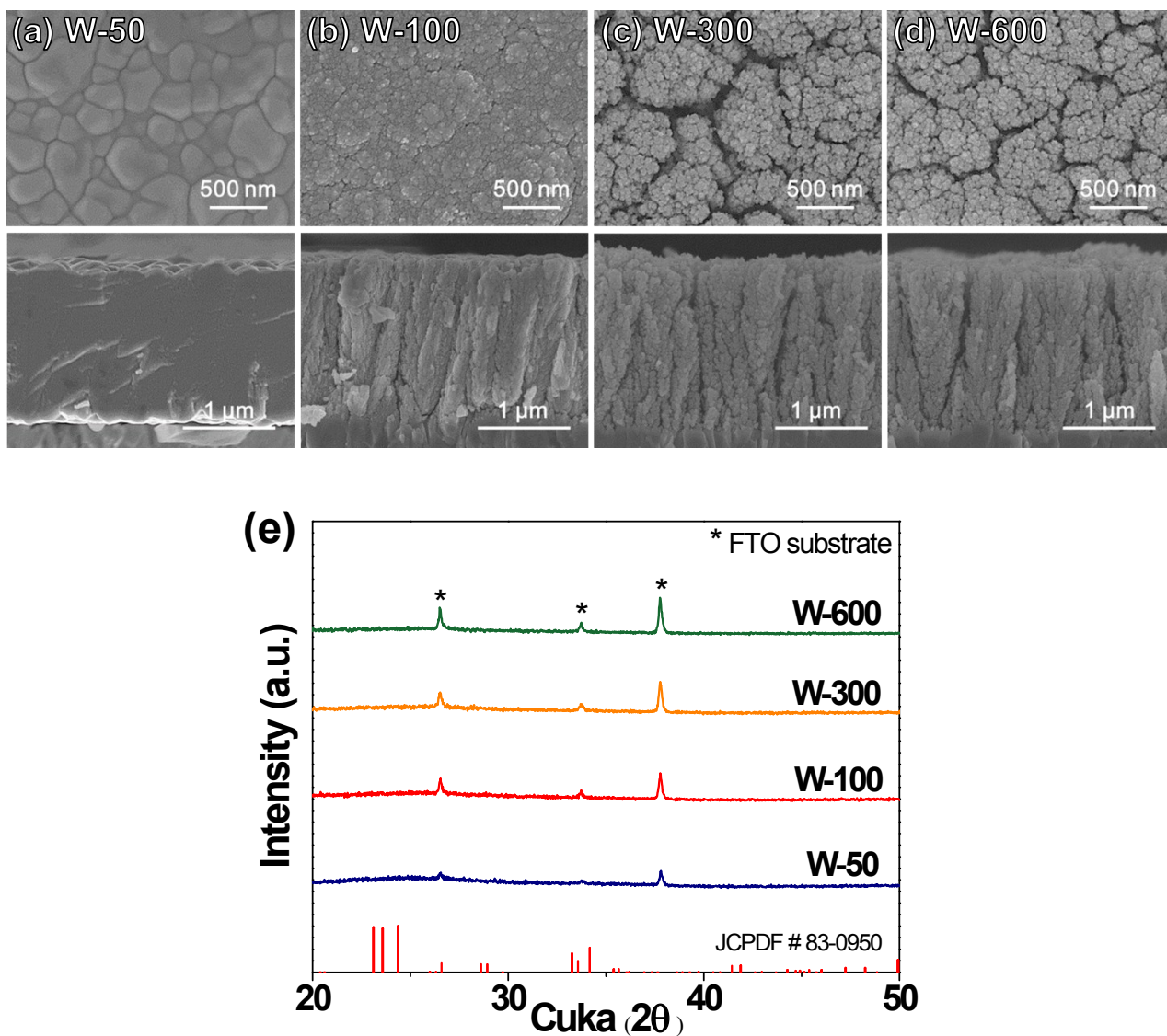


Figure S1. (a-d) Top and cross-sectional view SEM images and (e) XRD patterns of as-prepared WO<sub>3</sub> photoanodes deposited at oxygen working pressure of (a) 50 mTorr (deposition time=45min), (b) 100 mTorr (deposition time=30min), (c) 300 mTorr (deposition time=15min), and (d) 600 mTorr (deposition time=10min). The growth time was adjusted to tune the film thickness (1.8μm).

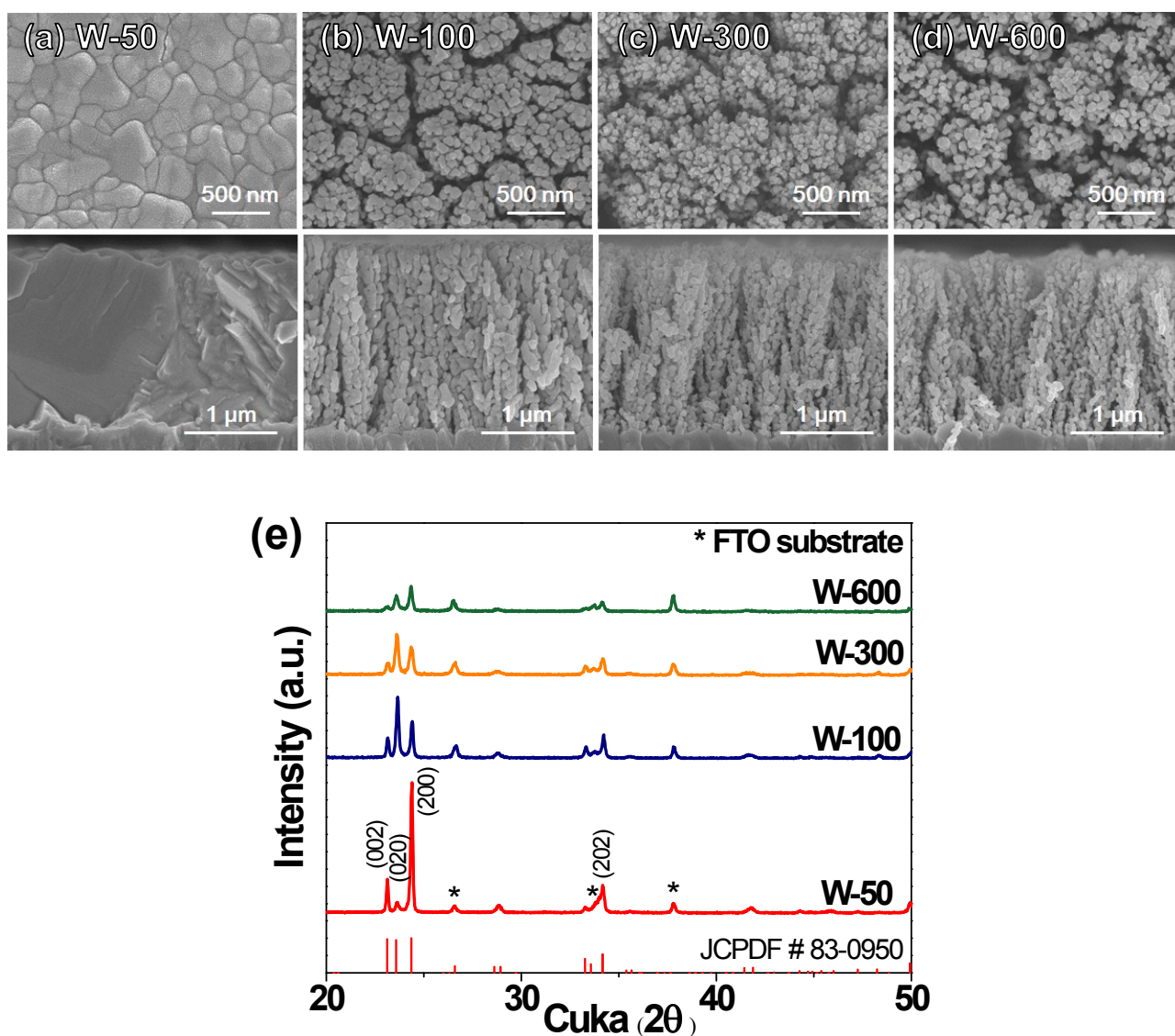
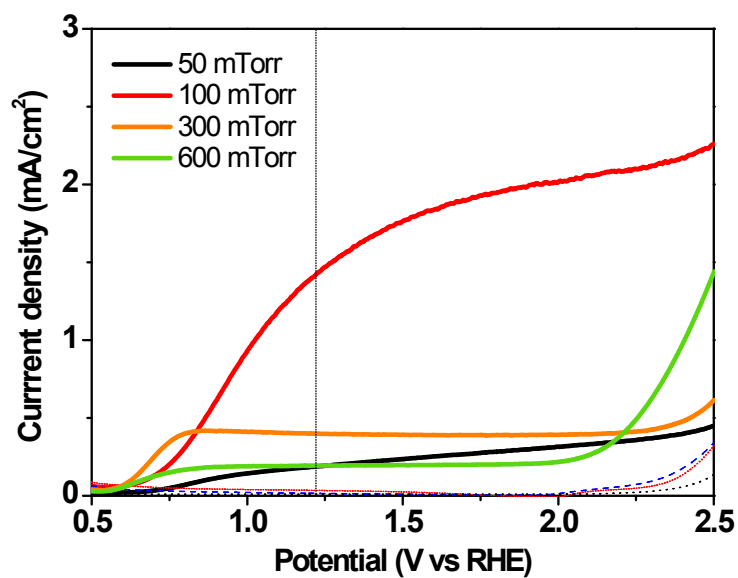
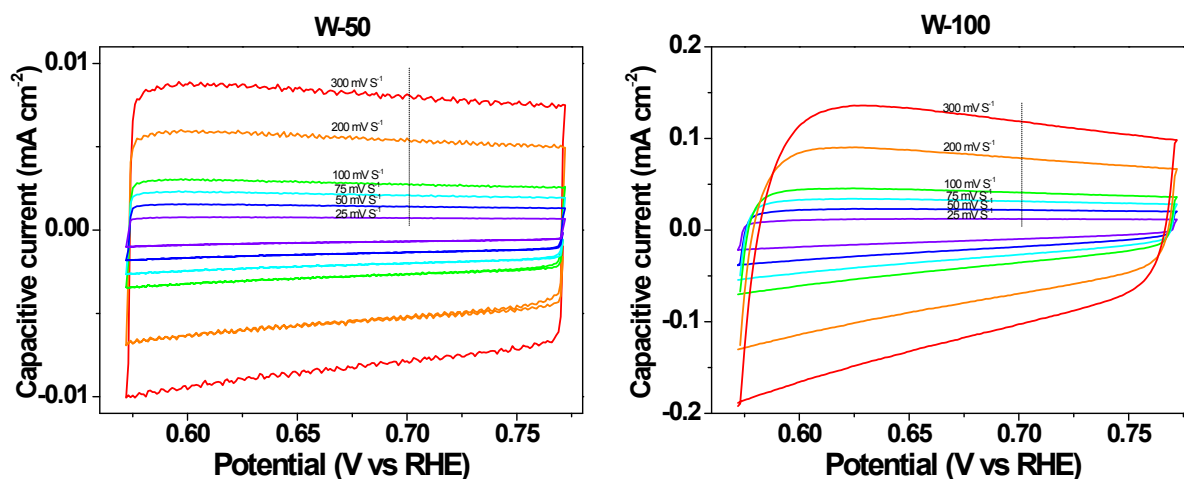


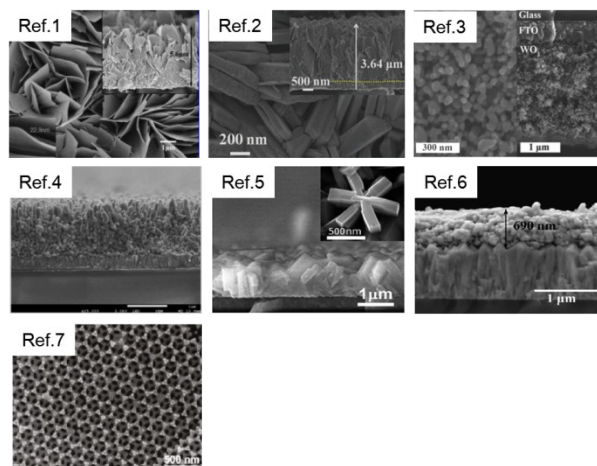
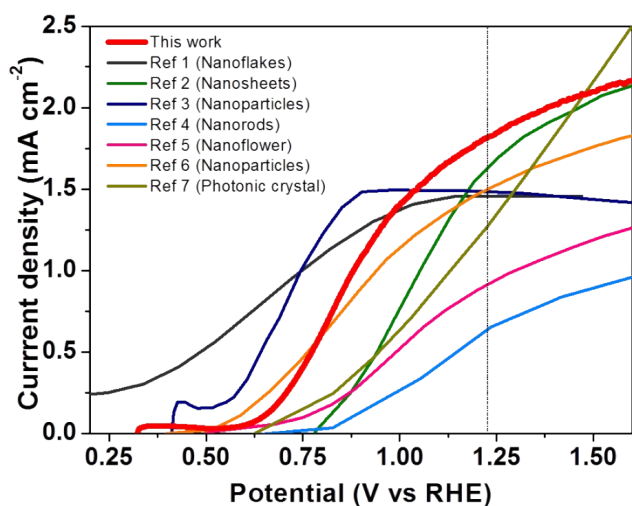
Figure S2. (a-d) Top and cross-sectional view SEM images, and (e) XRD patterns of WO<sub>3</sub> photoanodes after thermal annealing at 550 °C/2h, which are deposited at various oxygen working pressures. (a) 50 mTorr (deposition time=45min), (b) 100 mTorr (deposition time=30min), (c) 300 mTorr (deposition time=15min), and (d) 600 mTorr (deposition time=10min). \*The samples prepared at 300 and 600 mTorr are showing weak adhesion with FTO substrate so that those films are often detached or crushed during PEC measurements.



**Figure S3.** Photocurrent-potential (J-V) curves of WO<sub>3</sub> photoanodes (thickness=1.8 μm, after thermal annealing at 550 °C/2h). Most of samples synthesized at higher O<sub>2</sub> pressure, *i.e.*, 300mT and 600mT are detached or crushed during PEC measurements. Therefore, the much lower photocurrent densities of these samples may be attributed to the poor contact with FTO substrate.



**Figure S4.** Cyclic voltammograms of  $\text{WO}_3$  photoanodes (W-50 and W-100) measured at different scan rates (25-300 mV/sec). The sweep potential range, *i.e.*, (-0.05 - 0.15 V vs. Ag/AgCl  $\rightarrow$  0.57 - 0.77 V vs. RHE) was selected based on the previous report.<sup>1</sup> In this range, all current is only attributed to capacitive charging due to the absence of any redox features in the dark condition. Even though it is not possible to obtain a value of the true electrochemical surface area per projected geometric area without an atomically flat  $\text{WO}_3$  reference standard and detailed knowledge of the electronically accessible surface sites, we adopted this method and determined the relative electrochemical surface area by assuming that the intrinsic specific surface capacitance of all  $\text{WO}_3$  films is approximately the same.<sup>2</sup>



Refs	Morphology of WO <sub>3</sub> (Thickness, μm)	PEC measurement conditions			J <sub>ph</sub> @1.23V <sub>RHE</sub> (mA/cm <sup>2</sup> )
		Electrolyte (pH)*	Light source	Electrodes system	
Ref. 1 <sup>3</sup>	Nanoflakes (5.6)	0.1M Na <sub>2</sub> SO <sub>4</sub> (pH 3.0-7.0)	Solar simulator (1sun, 100mW/cm <sup>2</sup> )	Two electrodes (Pt counter)	1.45
Ref. 2 <sup>4</sup>	Nanosheets (3.64)	0.1M Na <sub>2</sub> SO <sub>4</sub> (pH 3.0-7.0)	Solar simulator (1sun, 100mW/cm <sup>2</sup> )	Three electrodes (Pt counter, Ag/AgCl ref.)	1.63
Ref. 3 <sup>5</sup>	Nanoparticles (2.3)	1 M H <sub>2</sub> SO <sub>4</sub> (pH ~0.0)	Solar simulator (1sun, 100mW/cm <sup>2</sup> )	Three electrodes (Pt counter, Hg/Hg <sub>2</sub> SO <sub>4</sub> saturated K <sub>2</sub> SO <sub>4</sub> ref.)	1.48
Ref. 4 <sup>6</sup>	Nanorods (1.58)	0.5 M Na <sub>2</sub> SO <sub>4</sub> (pH 3.0-7.0)	Solar simulator (1sun, 100mW/cm <sup>2</sup> )	Three electrodes (Pt counter, SCE ref.)	0.66
Ref. 5 <sup>7</sup>	Nanoflowers (0.6)	1 M H <sub>2</sub> SO <sub>4</sub> (pH ~0.0)	Solar simulator (1sun, 100mW/cm <sup>2</sup> )	Three electrodes (Pt counter, SCE ref.)	0.91
Ref. 6 <sup>8</sup>	Nanoparticles (0.69)	0.5 M H <sub>2</sub> SO <sub>4</sub> (pH ~0.0)	Solar simulator (1sun, 100mW/cm <sup>2</sup> )	Three electrodes (Pt counter, Ag/AgCl ref.)	1.50
Ref. 7 <sup>9</sup>	Inverse opal (2.6)	0.1 M Na <sub>2</sub> SO <sub>4</sub> (pH 3.0-7.0)	500W Xenon Lamp (250mW/cm <sup>2</sup> , 300-800nm)	Three electrodes (Pt counter, SCE ref.)	1.28
This work	Tree-like nanoporous (3.2)	Phosphate buffer (pH 7.0)	Solar simulator (1sun, 100mW/cm <sup>2</sup> )	Three electrodes (Pt counter, Ag/AgCl ref.)	1.82

**Figure S5.** Comparison of PEC performance with previous works. Photocurrent-potential (J-V) curves of WO<sub>3</sub> photoanodes and corresponding SEM images. Table summarizes WO<sub>3</sub> morphology and measurement conditions. \*Since all the reference papers doesn't mention the pH values, the pH values are referred from other papers.

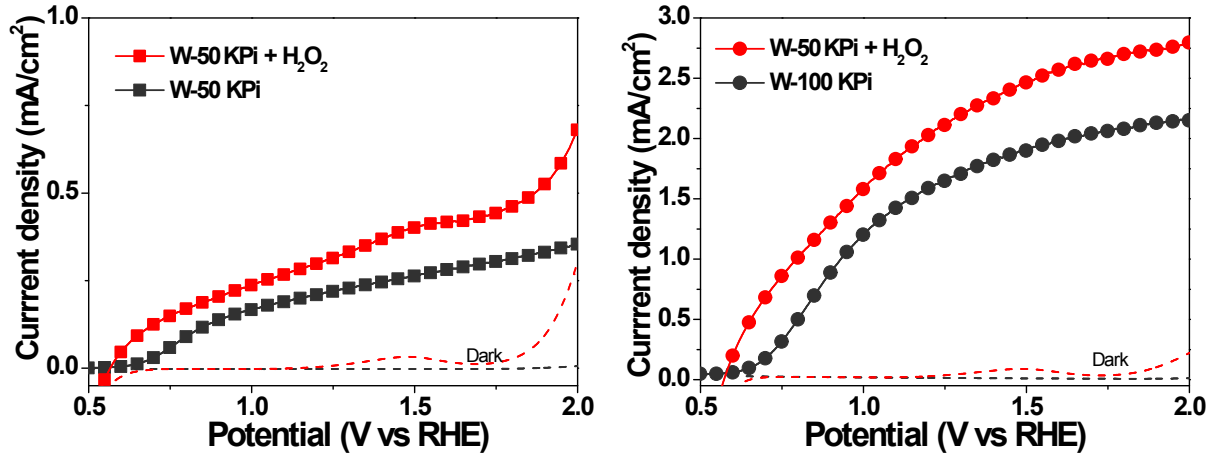


**Figure S6.** Photocurrent-potential (J-V) curves of W-50 and W-100 samples before and after addition of  $\text{H}_2\text{O}_2$  (5 vol.%).  $\text{Na}_2\text{SO}_3$  also gives similar results. The charge transport and transfer efficiencies were estimated as functions of applied potential by using  $\text{H}_2\text{O}_2$  or  $\text{Na}_2\text{SO}_3$  as hole scavenger under AM1.5G simulated solar light illumination. The key assumption for this approach is that the oxidation kinetics of  $\text{H}_2\text{O}_2$  or  $\text{Na}_2\text{SO}_3$  is very fast and its charge transfer efficiency is 100%, so the ratio of photocurrent density measured in  $\text{H}_2\text{O}$  and  $\text{H}_2\text{O}_2$  (or  $\text{H}_2\text{O}$  and  $\text{Na}_2\text{SO}_3$ ) give the charge transfer efficiency ( $\eta_{\text{transfer}}$ ) for  $\text{H}_2\text{O}$ . (Eq. 1) The charge transport efficiency ( $\eta_{\text{transport}}$ ) was further calculated by dividing photocurrent density in  $\text{H}_2\text{O}_2$  (or  $\text{Na}_2\text{SO}_3$ ) by the total light absorption efficiency ( $\eta_{e^-/h^+}$ ) which is obtained from integration of light absorption (Figure 3c) with respect to the AM1.5G solar light spectrum (Eq. 2).

$$\eta_{\text{transfer}} = \frac{J_{ph, \text{H}_2\text{O}}}{J_{ph, \text{H}_2\text{O}_2}} \quad (1)$$

$$\eta_{\text{transport}} = \frac{J_{ph, \text{H}_2\text{O}_2}}{\eta_{e^-/h^+}} \quad (2)$$



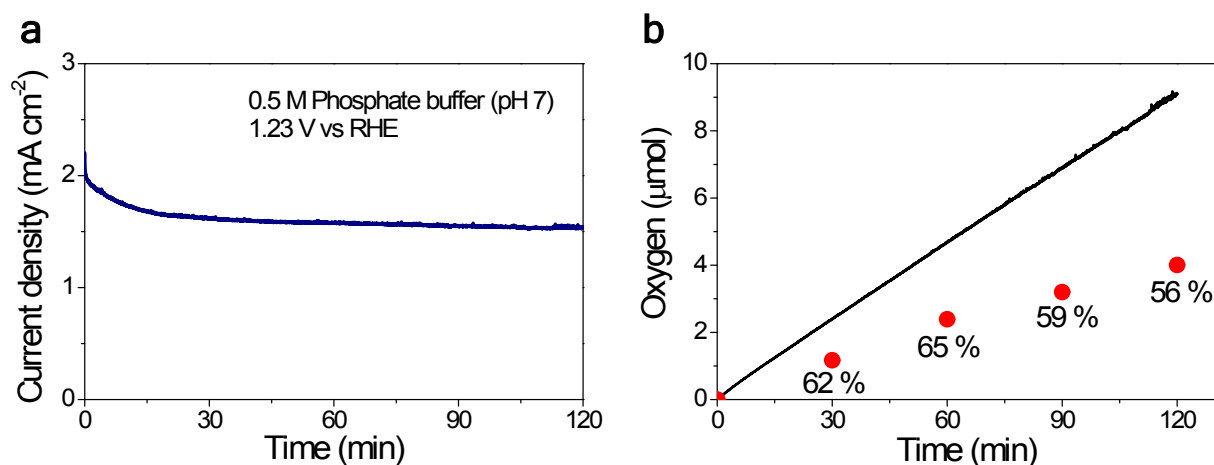


**Figure S7.** (a) Photocurrent-time (J-t) curves of W-100 photoanode measured at 1.23 V versus RHE in 0.5 M phosphate buffer solution under simulated solar light illumination (100mW/cm<sup>2</sup>). (b) Expected amounts of O<sub>2</sub> calculated from the photocurrent assuming 100% Faradaic efficiency (Black line) and actual amounts of O<sub>2</sub> produced (red circle). The numbers show calculated faradaic efficiencies at the given time.

## References

1. N. Wang, J. Zhu, X. Zheng, F. Xiong, B. Huang, J. Shi and C. Li, *Faraday Discussions*, 2014.
2. B. A. Pinaud, P. C. Vesborg and T. F. Jaramillo, *The Journal of Physical Chemistry C*, 2012, **116**, 15918-15924.
3. J. Su, X. Feng, J. D. Sloppy, L. Guo and C. A. Grimes, *Nano Letters*, 2011, **11**, 203-208.
4. D.-D. Qin, C.-L. Tao, S. A. Friesen, T.-H. Wang, O. K. Varghese, N.-Z. Bao, Z.-Y. Yang, T. E. Mallouk and C. A. Grimes, *Chemical Communications*, 2012, **48**, 729-731.
5. S. Hilaire, M. J. Suess, N. Kranzlin, K. Bienkowski, R. Solarska, J. Augustynski and M. Niederberger, *Journal of Materials Chemistry A*, 2014, **2**, 20530-20537.
6. Y. Liu, L. Zhao, J. Su, M. Li and L. Guo, *ACS Applied Materials & Interfaces*, 2015, **7**, 3532-3538.
7. N. Wang, D. Wang, M. Li, J. Shi and C. Li, *Nanoscale*, 2014, **6**, 2061-2066.
8. R. H. Gonçalves, L. D. T. Leite and E. R. Leite, *ChemSusChem*, 2012, **5**, 2341-2347.
9. X. Chen, J. Ye, S. Ouyang, T. Kako, Z. Li and Z. Zou, *ACS Nano*, 2011, **5**, 4310-4318.